

Photochemical Reaction of Ozone with 2-Iodopropane and the Four Polyfluoroiodoethanes C_2F_5I , CF_3CH_2I , CF_2HCF_2I , and CF_3CFHI in Solid Argon at 14 K. FTIR Spectra of the Iodoso-Intermediates ($Z-IO$), the Iodyl-Intermediates ($Z-IO_2$), and the Various Complexes $(CH_3)_2C=O\cdots HI$, $CF_3C(O)H\cdots XI$, $CF_2HC(O)F\cdots IF$, and $CF_3C(O)F\cdots XI$ (Where $X = H$ or F)

Robin J. H. Clark,* Jonathan R. Dann, and Loraine J. Foley

Christopher Ingold Laboratories, University College London, 20 Gordon Street, London WC1H 0AJ, U.K.

Received: July 2, 1997; In Final Form: September 18, 1997[⊗]

Deposition of ozone with either 2-iodopropane, pentafluoroiodoethane, 1,1,1-trifluoroiodoethane, 1,1,2,2-tetrafluoroiodoethane, or 1,1,1,2-tetrafluoroiodoethane, in an argon matrix at 14 K has been shown by FTIR spectroscopy to lead to the formation of a molecular complex. Irradiation of such complexes with near-infrared radiation led to the formation of the corresponding iodoso-species ($Z-IO$). Radiation of wavelengths > 410 nm produced bands typical of iodyl-species ($Z-IO_2$), while subsequent photolysis with UV-vis ($\lambda > 350$ nm) radiation led to the development of bands attributed to hypiodo-species ($Z-OI$) and to carbonyl complexes (carbonyl $\cdots XI$, where $X = H$ or F). Further photolysis using Pyrex- ($\lambda > 290$ nm) and quartz- ($\lambda > 240$ nm) filtered radiation increased the yield of the carbonyl complexes, which were the final products to be detected in the reaction series of each precursor with ozone. Sample annealing confirmed that the carbonyl complexes existed in two geometric arrangements, a molecular-pair type and a head-to-tail dipole-dipole type. In a similar study of each precursor deposited in a solid oxygen matrix the carbonyl complexes were the only species that could be identified. Thus by studying the reactions of ozone with these iodine-containing compounds it has been possible to extend the number of known species having $I-O_x$ bonds, to detect a number of carbonyl $\cdots XI$ complexes ($X = H$ or F), and to clarify the mechanisms of the reactions.

Introduction

To investigate the nature of atmospherically important reactions between halocarbons and ozone, earlier matrix isolation studies^{1–3} have been extended to include 2-iodopropane owing to its similarities to iodoethane. Detection of the various products is expected to enhance our understanding of the photochemical path involved in such reactions, and also to yield a number of novel species and complexes. A further extension is to the study in solid argon of the reactions of ozone and polyfluoroiodoethanes possessing $X-CF_2I$, $X-CH_2I$, and $X-CFHI$ backbones, viz. pentafluoroiodoethane, 1,1,1-trifluoroiodoethane, 1,1,2,2-tetrafluoroiodoethane, and 1,1,1,2-tetrafluoroiodoethane. The photochemical reactions of these four precursors with ozone are expected to produce the fluoro-analogues of the $-IO_x$, $-OI$, and carbonyl species reported in the reaction between iodoethane and ozone.⁴ For example, if iodoso-species ($Z-IO$) could be detected as products in each case, it should be possible to compare both their photochemical and spectral behavior with that of analogous species.^{1–3} It has been proposed that a five-membered ring intermediate⁵ is formed in the gas-phase reaction between ozone and iodoethane. An aim of this study is to provide evidence for a similar fluoro-intermediate. With iodoethane and pentafluoroiodoethane it is not possible to determine from which carbon atom, α or β , the H or F atoms in the products (HI , HOI , FI or FOI) come, but with 1,1,1-trifluoroiodoethane, CF_3CH_2I , this is possible; hence the presence or absence of a five-membered ring intermediate should be able to be established. Also, 1,1,2,2-tetrafluoroiodoethane, CF_2HCF_2I , has a hydrogen atom on the β -carbon atom and might thus produce HOI as a product, which would confirm the existence of a five-membered ring intermediate in the reaction path. The fluorinated iodoethanes also form a range of carbonyl $\cdots XI$ ($X = H$ or F) species. If the five-membered

ring intermediate were involved in the mechanism, then CF_3-CH_2I should produce the fluoroalkene $CF_2=CH_2$ and FOI . Subsequent oxygen atom addition, and H/F atom migration across the double bond would lead to the formation of either $CF_2HC(O)F$ or $CH_2FC(O)H$ as the final carbonyls, the detection of either of which would also clarify the mechanism. Whichever carbonyl is produced, it is expected to form a complex with the remainder of the precursor, e.g. in the case of 1,1,1,2-tetrafluoroiodoethane, CF_3CFHI , to form, finally, either $CF_3C(O)F\cdots HI$ or $CF_3C(O)H\cdots IF$. The wavenumbers of the bands assigned to these carbonyl complexes could be compared with those of other carbonyl $\cdots XI$ complexes (where $X = H$ or F) in order to identify the species involved in the mechanism.

The polyfluoroiodoethanes undergo a variety of further reactions; thus the gas-phase photolysis of perfluoroiodoalkanes, $CF_3(CF_2)_nI$, in oxygen produces carbonyl difluoride, COF_2 .⁶ Photolysis of trifluoroiodomethane in an oxygen/argon matrix produces the radical CF_3O ,⁷ while photolysis of ozone and tetrafluoroethene⁸ produces carbonyl fluoride as the prime product via $C=C$ bond rupture and addition of an oxygen atom to the CF_2 species. It has, moreover, been shown that O_2 can add to CF_3 to form CF_3O_2 .^{9,10} Thus photolysis of these polyfluoroiodoethanes may produce different products from those expected by simple extrapolation from the results reported for iodoethane.

Experimental Section

The infrared spectra were recorded on a Bruker IFS 113v Fourier-transform infrared spectrometer over the range 500–4000 cm^{-1} at a resolution of 1 cm^{-1} using a germanium-coated KBr beam splitter and a MCT detector cooled with liquid nitrogen. The matrices were scanned 500 times, the interferograms being coadded and converted to a single beam spectrum by a fast Fourier transform algorithm using a zero filling factor of times four. The spectrum was converted to a double-beam

[⊗] Abstract published in *Advance ACS Abstracts*, November 15, 1997.

TABLE 1: Infrared Bands/cm⁻¹ Detected for 2-Iodopropane (Group 1) in a Number of Matrices

Ar	¹⁶ O ₃ /Ar	¹⁸ O ₃ /Ar	assignment
3007.0w	3006.6mw	3008.0s	ν_a CH ₃
	2991.3mw	2989.2m	
2987.5w	2986.6mw	2986.4ms	
	2982.2mw	2983.0ms	
2966.2m	2966.2mw	2966.7s	
2928.9m	2929.0m	2929.1vs	ν_s CH ₃
	2924.3mw	2924.1sh, m	
2916.4w	2918.7w	2918.5wm	
		2912.9wm	
2901.2w	2902.7w	2902.5w	ν CH ₃
2886.9w	2887.7w	2892.5m	
2875.3mw	2879.2w	2878.4mw	
	2867.7w	2868.4mw	
1464.4m	1463.3m	1463.1s	δ_a CH ₃
		1458.7mw	
1455.0m	1453.8m	1453.4ms	
	1448.1w	1448.4mw	
1387.0m	1386.2m	1386.1m	δ_s CH ₃
1371.9m	1372.5ms	1372.1vs	
1210.9s	1211.6s	1211.6vw	ν C-C
1208.0s	1207.8s	1207.8vs	
		1188.7m	
1148.0s	1149.1vs	1149.0vs	δ CH ₃
		1144.9sh, mw	
1137.2vw	1137.7w	1137.9w	
		1133.3w	ρ_{o-o-p} CH ₃
1119.9vw	1120.0w	1121.7w	
		1061.4w	ρ_{i-p} CH ₃
		1050.8w	
	928.2w	928.3mw	ρ_{i-p} CH ₃
876.4m	875.8m	875.6s	
584w, br		588.7w	ν C-I
		582.5w	
548.9w		550.7w	
		547.3w	

absorbance spectrum. The wavenumbers of the bands observed are accurate to ± 0.2 cm⁻¹.

Ozone was generated from either research grade oxygen (>99.99%) or oxygen-18 (>97.7%) supplied by British Oxygen Co. and Enritech Enrichment Technologies Ltd., respectively, or from a mixture of each. Argon, 2-iodopropane, pentafluoroiodoethane, 1,1,1-trifluoroiodoethane, 1,1,2,2-tetrafluoroiodoethane and 1,1,1,2-tetrafluoroiodoethane were used as supplied by Aldrich, and, excluding argon, were degassed by multiple freeze-thaw cycles with liquid nitrogen prior to use. The halocarbons were then diluted separately at species-to-argon (S/Ar) ratios in the range 1:200 to 1:600. The precursors were then separately deposited for 8 h at rates of approximately 3 mmol h⁻¹ onto the CsI cold window (14 K) of a Displex closed-cycle helium cryostat (Air Products DE 202 S).^{11,12} The vacuum shroud surrounding the cold window can be aligned for infrared transmission studies, for gas deposition and for sample photolysis. Spectra were recorded after each matrix irradiation or warming cycle to ca. 30 K in order to monitor changes caused by these processes.

The matrices were photolyzed for varying periods of time with an Oriel xenon mercury lamp, a 5 cm thick water filter being placed between the lamp and the sample to reduce the infrared output of the lamp. The matrices were photolyzed with various bands of near-infrared, visible, and ultraviolet radiation by use of the following transmission filters: infrared 4 mm thick green ($\lambda > 800$ nm), 8 mm thick deep red ($\lambda > 650$ nm), 2 mm thick yellow ($\lambda > 550$ nm), 2 mm thick green ($\lambda > 450$ nm), 2 mm thick green ($\lambda > 410$ nm), Corning 7 mm blue/green (550 > $\lambda > 350$ nm), Pyrex ($\lambda > 290$ nm) and quartz ($\lambda > 240$ nm). In this way the threshold wavelength of formation of each photoproduct could be established.

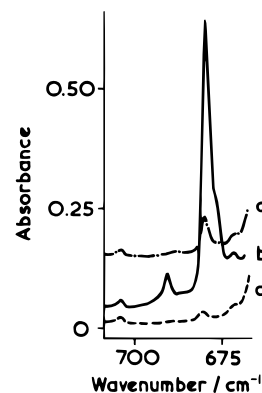


Figure 1. Infrared spectra in the ν_{10} region of a matrix containing 2-iodopropane/¹⁸O₃/Ar (1:6:700) after (a) deposition, (b) infrared-photolysis ($\lambda > 650$ nm), and (c) UV-vis photolysis ($\lambda > 350$ nm). The spectra show the band attributed to the I¹⁸O stretch of 2-iodopropane, (CH₃)₂CHIO (group 2).

Results

A. 2-Iodopropane and Ozone in Argon. The spectrum of an argon matrix containing 2-iodopropane ((CH₃)₂CHI/Ar = 1:500) was recorded, and the major bands were assigned (Table 1) using those for isopropane as a guide.¹³ Co-deposition of 2-iodopropane and ozone in an argon matrix ((CH₃)₂CHI/O₃/Ar = 1:6:800), and the subsequent photolysis or warming of the matrix, produced several bands which are grouped in Tables 1–5 according to their photolytic and thermal behavior in the matrix.

Bands detected after co-deposition of 2-iodopropane and ozone in an argon matrix (group 1 bands) resemble those assigned to 2-iodopropane (Table 1) and ozone,¹⁴ the biggest wavenumber shifts occurring for the ozone bands. Variation of the (CH₃)₂CHI/O₃/Ar ratio had no effect on the products detected.

Bands generated by photolysis of a matrix containing ozone and 2-iodopropane using $\lambda > 800$ nm radiation resulted in the growth of new bands (group 2 bands) at the expense of the group 1 bands. Further photolysis with > 650 nm radiation doubled the intensities of the group 2 bands; the intensities were doubled again by > 410 nm excitation. However, group 2 bands themselves were destroyed by $\lambda > 350$ nm radiation to produce groups 4 and 5 bands. Group 2 bands include medium and weak bands at 1200.1 and 1158.9 cm⁻¹ assigned to perturbed C–C–H bends, a medium band at 714.5 cm⁻¹ (¹⁸O at 690.8, 679.8 and 671.8 cm⁻¹) assigned to an I–O vibration (Table 2, Figure 1) on the basis of the ¹⁸O-shift of 34.7 cm⁻¹ and a weak band at 551.2 cm⁻¹ assigned to a C–I stretch (Table 2).

Group 3 bands were first detected very weakly after near-infrared ($\lambda > 650$ nm) photolysis. Further visible ($\lambda > 410$ nm) and $\lambda > 350$ photolysis increased their intensities by 20 and 25%, respectively, whereas photolysis with Pyrex- and quartz-filtered radiation reduced the intensities. Group 3 bands (Table 3 and Figure 2) occur between 833.0 and 792.7 cm⁻¹, with the ¹⁸O isotopomer bands occurring between 794.0 and 747.2 cm⁻¹. Based on the ¹⁸O-shifts of ~ 40 cm⁻¹ and shifts between symmetric and antisymmetric stretches of ~ 34 cm⁻¹, these bands are assigned to IO₂ stretching modes.

Group 4 bands are detected after photolysis of the matrix with $\lambda > 350$ nm radiation, coinciding with the loss of the group 2 bands; group 4 bands are destroyed by Pyrex-filtered photolysis. Weak bands belonging to this group (Table 4) are detected at 3446.4 and 3445.3 cm⁻¹. On the basis of the ¹⁸O-shifts (3.5 and 10.8 cm⁻¹ respectively) and the wavenumbers,⁴ these bands clearly arise from O–H stretches. The other weak

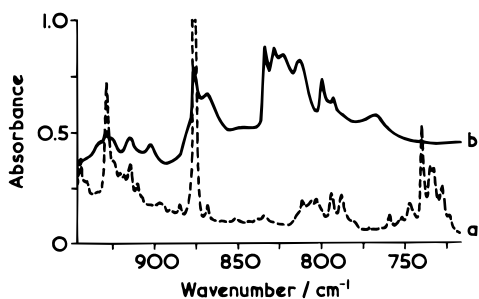
TABLE 2: Infrared Bands/cm⁻¹ Assigned to the Iodoso-Species (Z-IO), (Group 2), Detected after Photolysis ($\lambda > 650$ nm) of Ozone and (CH₃)₂CHI, C₂F₅I, CF₃CH₂I, CF₂HCF₂I, and CF₃CFHI in Argon at 14 K

(CH ₃) ₂ CHIO	C ₂ F ₅ IO	CF ₃ CH ₂ IO	CF ₂ HCF ₂ IO	CF ₃ CFHI	assignment
714.5m	738.7w	732.4mw 727.1vw	739.5w 734.4w 727.6w 722.3w	732.0w 726.0w	ν I ¹⁶ O
690.8w 679.8m 671.8sh, w 551.2w	706.9w	695.2w 688.7vw	691.4vw 680.6vw	694.6w	ν I ¹⁸ O
	535.3vw 527.2vw	554.0w 543.1w	534.4w	549.6vw 547.7vw	ν C-I

TABLE 3: Infrared Bands/cm⁻¹ Assigned to the Iodol-Species (Z-IO₂), (Group 3), Detected after Photolysis of Argon Matrices Containing Ozone and (CH₃)₂CHI ($\lambda > 650$ nm), C₂F₅I ($\lambda > 350$ nm), CF₃CH₂I ($\lambda > 410$ nm), CF₂HCF₂I,^a and CF₃CFHI ($\lambda > 350$ nm)

(CH ₃) ₂ CHIO ₂	C ₂ F ₅ IO ₂	CF ₃ CH ₂ IO ₂	CF ₃ CFHI ₂	assignment
833.0m	818.7vw ^b	815.5w	815.8br, vw	ν_a I ¹⁶ O ₂
827.7ms	812.1w	811.4vw ^b	810.2w	
820.7m	807.6vw	809.4w	809.3vw ^b	
813.7m	799.9vw	808.4vw ^b	805.1w	
		806.9vw	801.1w ^b	
807.9w ^b		787.5vw ^b	787.9w ^b	ν_a I ¹⁶ O ¹⁸ O
803.2w ^b		783.3vw ^b	782.8vw ^b	
		781.0vw ^b		
799.0m	c		777.1vw ^b	ν_s I ¹⁶ O ₂
795.0m				
792.7m				
794.0mw	768.6mw ^b	773.9vw	768.0vw ^b	ν_a I ¹⁸ O ₂
788.2mw	764.7mw ^b	768.3vw ^b	768.0vw	
	759.2mw ^b	768.0vw		
		765.9vw		
		764.5vw ^b		
		753.7vw ^b	759.4vw ^b	ν_s I ¹⁶ O ¹⁸ O
		752.2vw ^b	757.5vw ^b	
759.6mw	d	732.0vw	747.2vw ^b	ν_s I ¹⁸ O ₂
755.6w			746.2vw	
752.3mw			742.1vw ^b	
747.2mw			741.6w	
			735.7w	

^a No bands detected in this region for the iodol-species of this precursor. ^b Bands detected using ozone prepared from a ca. 1:1 mix of ¹⁶O₂ and ¹⁸O₂. ^c Obscured by bands due to OCF[•] bend of product group 5. ^d Obscured by bands due to C-C stretch of precursor.

**Figure 2.** Infrared spectra in the region 950–725 cm⁻¹ after UV-vis ($\lambda > 350$ nm) photolysis of matrices containing (a) 2-iodopropane/¹⁸O₃/Ar (1:6:800) and (b) 2-iodopropane/¹⁶O₃/Ar (1:6:700). The spectra show the bands assigned to the group 3 species, 2-iodylpropane, (CH₃)₂-CHIO₂.

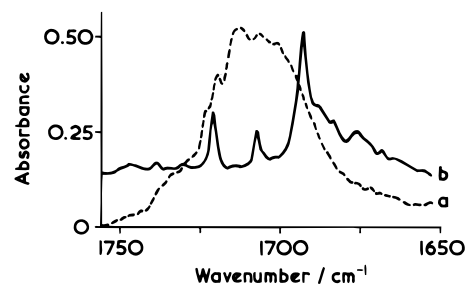
band in this group at 578.8 cm⁻¹ (¹⁸O-shift of 27.8 cm⁻¹) is assigned to an O-I vibration.

The bands assigned to group 5 (Table 5) were first detected after photolysis with $\lambda > 350$ nm radiation; Pyrex- and quartz-filtered irradiation increased their intensities. Bands detected between 1723.2 and 1700.3 cm⁻¹ are assigned to carbonyl stretches (Figure 3).

TABLE 4: Infrared Bands/cm⁻¹ Assigned to the Hypoiodo-Species (Z-OI), (Group 4), or Hydrogen Hypoiodide (HOI), Detected after Photolysis ($\lambda > 350$ nm) of Ozone and (CH₃)₂CHI, C₂F₅I, and CF₃CH₂I in Argon Matrices at 14 K^a

(CH ₃) ₂ CHI + O ₃	C ₂ F ₅ I + O ₃	CF ₃ CH ₂ I + O ₃	assignment
3446.4w		3492.3w ^b	ν ¹⁶ O-H
3445.3w		3444vw	
3442.9w			ν ¹⁸ O-H
3434.5w			
	968.7m		ν C- ¹⁶ O
	961.5m		
	955.7mw		ν C- ¹⁸ O ?
	953.3mw		
578.8w	583.9w	588.2vw 577.7vw 567.4vw	ν ¹⁶ O-I
551.0mw	578.6mw ^c		ν ¹⁸ O-I

^a No hypoiodo-type bands detected for the reaction of ozone with CF₂HCF₂I or CF₃CFHI. ^b Band formed after quartz filtered ($\lambda > 240$ nm) photolysis of CF₃CH₂I in an oxygen matrix. ^c Assignment uncertain, possibly due to either ν ¹⁸O-I or to ν ¹⁶O-I of FOI.

**Figure 3.** Infrared spectra in the $\nu_{C=O}$ region of acetone...HI complex, detected after Pyrex-filtered ($\lambda > 290$ nm) irradiation of matrices containing 2-iodopropane/ozone/Ar (1:6:800). Spectrum of (a) normal isotopic ozone $\sim 99\%$ ¹⁶O₃ and (b) the ¹⁸O isotopomer generated from ¹⁸O₃ ($\geq 97\%$ ¹⁸O₂).

B. Pentafluoroiodoethane and Ozone in Argon. After deposition of pentafluoroiodoethane in solid argon (C₂F₅I/Ar = 1:400) or in solid oxygen (C₂F₅I/O₂ = 1:200) matrices at 14 K, the bands detected (Table 6) were found to be at similar wavenumbers to those detected previously for liquid pentafluoroiodoethane.¹⁵ Ultraviolet ($\lambda > 240$ nm) photolysis of C₂F₅I isolated in argon for periods of up to 1 h produced no detectable new bands. This supports the assumption that the reactions occur as a result of treating ozone or excited oxygen molecules with pentafluoroiodoethane and not with some photodissociation product thereof.

Co-deposition of pentafluoroiodoethane (C₂F₅I/Ar = 1:200 to 1:400) and ozone (O₃/Ar = 1:200 to 1:1000) in an argon matrix, and subsequent photolysis or warming, produced a number of new bands which were grouped according to their behavior after wavelength- and time-dependent photolysis or annealing.

Group 1 bands were detected after co-deposition of pentafluoroiodoethane and ozone in an argon matrix, and resemble those

TABLE 5: Infrared Bands/cm⁻¹ Assigned to the Acetone...HI Species (Group 5), Formed after Photolysis of 2-Iodopropane and Ozone in Argon at 14 K, and Those Assigned to Acetone²⁸ and the Acetone...HF Species²⁷ in Argon

acetone ²⁸	acetone...HF ²⁷	¹⁶ O ₃ /Ar	¹⁸ O ₃ /Ar	assignment
1725	1715	1723.2sh,mw 1719.2sh, m 1712.9m 1706.9mw	1706.8w 1693.0mw 1687.7w 1683.2w	$\nu_{C=O}$
1430	1423	1453.5mw 1448.5mw 1444.0w 1422.1br, w 1419.0br, w	1442.8w 1439.3w 1426.1w	$\delta_a CH_3$
1363	1374	1386.2mw 1363.9w 1358.9vw 1355.8vw 1351.3vw	1381.4w 1377.1w 1362.8mw 1354.6w 1311.1w	$\delta_s CH_3$
1217	1242		1231.6w 1227.7w 1226.1w 1222.7w 1218.8w 1200.3m 1158.9m	ν_{C-C} δ_{CH_3}
1090	1097	1109.3w 1105.2w 1096.2w 933.6w 928.3w 925.0w 914.0w 902.0w	1110.8w 1106.4mw 1101.6w 923.0mw 914.3w 910.3w	$\rho_{o-o-p} CH_3$ ω_{CH_3} ω_{CH_3}
880		875.7m 868.3m 767.7mw		$\rho_{i-p} CH_3$ ν_{C-C}
529	556	630.9w 621.9w		$\delta_{C-C=O}$

detected in the spectra of pentafluoroiodoethane (Table 6) and of ozone¹⁴ isolated separately in argon. The biggest wavenumber shifts occur for the ozone bands at 1039.5, 1033.8 and 1032.0 cm⁻¹. In the mixed-ozone experiments, ¹⁶O_{3-x}¹⁸O_x bands are assigned to the ν_2 and ν_3 fundamentals and to the combination $\nu_1 + \nu_3$ of the six isotopomers of ozone (e.g. 16-16-16, 16-18-16 etc.). Group 1 bands reduced in intensity after near-infrared ($\lambda > 650$ nm) photolysis of the matrix.

Weak bands (group 2) were formed after photolysis with $\lambda > 650$ nm radiation, but with visible radiation ($\lambda > 550$ nm and $\lambda > 410$ nm) the band intensities increased by 30% after each successive 30 min cycle. However $\lambda > 350$ nm radiation of the matrices destroyed the bands. Group 2 included a strong band assigned to a perturbed CF₂ stretch at 1090.7 cm⁻¹, having a small ¹⁸O-shift of 1.5 cm⁻¹. Weak bands assigned to perturbed stretches of the CF₂I unit were detected at 902.6 and 897.3 cm⁻¹, and exhibited small ¹⁸O-shifts of < 0.9 cm⁻¹. A weak band at 738.7 cm⁻¹ (Figure 4) having an ¹⁸O-shift of 31.8 cm⁻¹, is assigned to the I-O stretch (Table 2). In the mixed-ozone experiments very weak bands detected between 638.1 and 615.5 cm⁻¹ and at 535.3 and 527.2 cm⁻¹ are assigned to CF₃ bends and perturbed C-I stretches (Table 2), respectively. Additionally, in the mixed-ozone experiments a band was detected at 738.2 cm⁻¹.

Group 3 bands (weak) were formed after $\lambda > 350$ nm photolysis (Table 3), and they remain unchanged on subsequent shorter wavelength irradiation ($\lambda > 240$ nm). Weak bands were detected in the ¹⁶O₃ experiment at 812.1, 807.6, and 799.9 cm⁻¹ (between 818.7 and 759.2 cm⁻¹ in the mixed ozone experiment,

TABLE 6: Infrared Bands/cm⁻¹ Detected for Pentafluoroiodoethane in a Variety of Matrices after Deposition at 14 K

Ar	O ₂	¹⁶ O ₃ /Ar	¹⁸ O ₃ /Ar	assignment
1335.2w	1334.2mw	1335.2m	1335.2m	$\nu_{CF_3} + \rho_{CF_2I}$
1324.1vs	1322.1s	1323.1vs	1322.4vs	ν_{CF_3}
1309.6w	1310.1mw	1310.1m	1309.6m	
1298.5w	1298.0mw	1298.5mw	1299.0mw	$\nu_{CF_3} + \tau$
		1289.3mw	1288.9m	
1286.9mw	1286.0ms	1287.4s	1286.9m	$\nu_{CF_2I} + \rho_{CF_2} ?$
1281.6w		1282.6ms	1283.1m	
1251.7w	1251.3mw	1251.7m	1251.7m	ν_{CF_3}
		1231.5sh	1234.9s	
			1230.0s	
1224.3vs	1219.0vs	1213.2vs	1212.2vs	
1198.2mw	1196.8m	1198.2ms	1197.7m	$\nu_{CF_2I} + \delta_{C-C-I} ?$
1182.3mw	1188.1mw	1181.8s	1181.8s	$\nu_{CF_2} + \tau$
		1181.3m	1177.5m	
1155.5vs	1153.6vs	1154.5vs	1167.4mw	ν_{CF_2}
1141.8mw	1142.8br, vs	1141.3vs	1152.9vs	
			1140.8s	
1105.6vs	1138.4vs	1137.0s	1136.0s	ν_{CF_2}
	1102.5vs	1104.6vs	1103.2vs	
		1097.9vs		
		1097.0s		
1083.5w	1082.5mw	1083.5m	1083.0m	$\nu_{CF_2I} + \rho_{CF_2I} ?$
1064.2w	1064.6w	1064.6mw	1064.6mw	
924.3vs	915.7vs	923.4sh		ν_{CF_2I}
919.5vs	907.0w	916.4vs	917.1vs	
897.3w	898.3m	897.3m	897.1m	
745.4vs	745.0s	745.9vs	745.4s	ν_{C-C}
		740.6m	737.7w	
729.1w	730.0m	729.1m	729.1m	$2\delta_{CF_2}$
623.0m	622.5s	624.4s	624.4s	δ_{CF_3}
590.7mw	590.7mw	591.1m	591.1m	
543.2s	543.0s	543.9br, vs	544.4s	

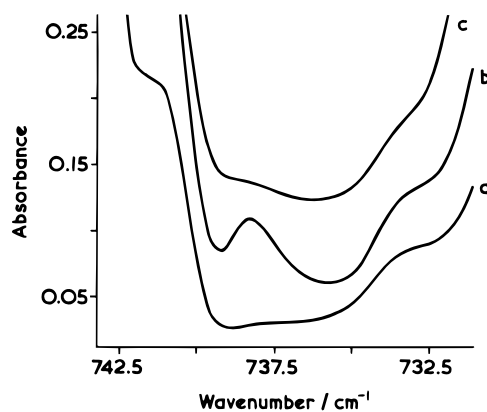


Figure 4. Infrared spectra in the range 742.5 and 732.5 cm⁻¹ of a matrix containing pentafluoroiodoethane and ozone in argon after (a) deposition at 14 K, (b) near-infrared photolysis ($\lambda > 650$ nm) and (c) UV-vis ($\lambda > 350$ nm), showing the ν_{IO} band of the group 2 species, iodosopentafluoroethane.

¹⁶O_{3-x}¹⁸O_x). The bands are considered to be characteristic of an IO₂ unit, based on the assignment methods⁴ for an iodyl-species, e.g. $\nu_a IO_2 - \nu_s IO_2 \sim 34$ cm⁻¹, while the ¹⁸O-shifts ~ 40 cm⁻¹.

Like the group 3 bands, group 4 bands were formed after UV-vis photolysis ($\lambda > 350$ nm) (Table 4) but, due to the low intensities, no change in band intensity could be distinguished after subsequent photolysis at shorter wavelength. This group consists of medium bands assigned to C-O stretches detected at 968.7 and 961.5 cm⁻¹, having ¹⁸O-shifts of 13.0 and 8.2 cm⁻¹, respectively. Weak bands at 583.9 cm⁻¹ and at 584.4, 581.0 and 577.4 cm⁻¹ in the mixed-ozone experiments are assigned to O-I stretches.⁴

The bands detected for group 5 were first detected after UV-vis irradiation; Pyrex-filtered photolysis nearly quadrupled the

TABLE 7: Infrared Bands/cm⁻¹ of Group 5 Species, CF₃C(O)F···IF, Detected after UV–Vis Photolysis (λ > 350 nm) of Pentafluoroiodoethane with Ozone in an Argon Matrix and in a Solid Oxygen Matrix

O ₂	¹⁶ O ₃ /Ar	¹⁸ O ₃ /Ar	assignment ^a
1935.0vw	1938.4ms	1904.7m	ν _{C=O}
	1936.4ms	1903.4m	
	1933.9ms		
1905.1mw	1909.9ms	1875.7s	
1903.6mw	1907.7s		
	1905.9s	1862.8mw	
	1901.2sh, s	1854.4mw	
1887.7w	1886.8mw	1850.4sh, w	
	1327.0vs		ν _{CF₃}
	1286.5s	1276.8m	
	1282.6s	1275.8m	
1251.3mw	1267.2s	1267.6s	ν _{FCF₂}
	1250.8vs	1259.0vs	
		1240.6s	
1196.8ms	1197.7vs	1197.7s	ν _{F–C–F}
		1192.9s	
1180.9s	1166.0vs	1181.8s	δ _{O–C–F} + ω _{i–ph} ?
1173.6ms		1177.5s	
		1167.4m	
1100.6vs	1091.2vs	1089.2s	ν _{C–F}
1082.5m	1082.5s	1083.0s	δ _{CF₃} + ρ _{i–ph} ?
	1067.6m	1068.5s	
	1063.7m	1064.6s	
		819.7w	ν _{C–C}
		807.6w	
771.5w	769.6m	768.7w	δ _{O–C–F}
763.8w	762.3mw	765.2w	
		758.9mw	
694.8vw		687.1w	δ _{CF₃}
688.1vw			
	644.7w		ω _{i–ph} + ω _{o–ph} ?
	596.5w	604.7w	ν _{sI–F}

^a Subscript i-ph = in-phase, subscript o-ph = out-of-phase.

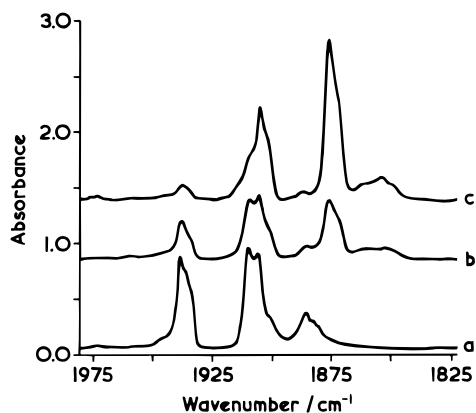


Figure 5. Infrared spectra in the ν_{C=O} region of the complex CF₃C(O)F···IF (group 5), detected after quartz-filtered photolysis of an argon matrix containing pentafluoroiodoethane and (a) ozone ¹⁶O₃, (b) mixed-ozone ¹⁶O_{3-x}¹⁸O_x and (c) ¹⁸O₃ showing the ¹⁶O- and ¹⁸O-isotopomers.

intensities, while quartz-filtered irradiation increased the intensities by a further 50% (Table 7). The most diagnostic bands for this group occur in the carbonyl stretching region (Figure 5). After the matrix was warmed, the intensity of the band at 1886.8 cm⁻¹ increased by 10%, at the expense of a 10% decrease in the bands centered around 1936 cm⁻¹. Similar behavior was noted for the bands of the ¹⁸O-isotopomer.

Pentafluoroiodoethane in Oxygen. The spectrum of pentafluoroiodoethane deposited in solid oxygen (C₂F₅I/O₂ = 1:100) resembles closely that in solid argon (Table 6). Photolysis of the matrices with quartz-filtered radiation was required before any new bands could be detected (Table 7); the latter resemble the group 5 bands.

TABLE 8: Infrared Bands/cm⁻¹ Detected after Deposition of 1,1,1-Trifluoroiodoethane in a Variety of Matrices at 14 K

Ar	O ₂	¹⁶ O ₃ /Ar	¹⁸ O ₃ /Ar	assignment
3052.3w	3055.6w	3048.3w	3054.1w	ν _a CH ₂
2998.9w	2996.7w	2990.0w	2990.0w	ν _s CH ₂
1469.6w	1469.2m	1469.7wm	1470.6w	δ _{CH₂}
1424.8ms	1427.2s	1425.3s	1426.3s	
	1404.6w	1408.0w	1406.5vw	
1378.1w	1375.2mw	1376.6w	1381.4vw	ρ _{CH₂} + δ _{CF₃}
	1356.4mw	1359.3w	1361.7w	
1349.2w	1345.8mw	1344.3w	1349.1w	
1290.0br, vs	1291.8vs	1291.3s	1292.2vs	ω _{CH₂}
1260.0vs	1262.8vs	1263.3s	1265.2vs	ν _{CF₃}
	1240.2w	1239.7w	1240.4vw	
1214.8s	1214.1s	1214.6s	1215.1s	ν _{C–F}
	1197.7w	1196.3w	1196.8vw	
1143.1s	1142.3s	1143.2mw	1144.2mw	ν _s CF ₃
1131.4m	1131.2s	1131.7m	1132.2m	ν _{C–F}
1117.2s	1116.2vs	1114.3vs	1118.2vs	
	1093.6wm		1094.5w	
1053.9s	1055.5vs	1054.0s	1058.9s	δ _{CH₂}
			1055.0vs	
842.6m	841.4s	842.4m	846.2w	ν _{C–C}
			842.8mw	
674.3m	674.1s	674.1m	675.5m	ν _{C–I}
629.2s	628.3s	629.2s	629.7s	δ _{CF₃}
532.1w	534.7w	534.7w	535.2w	
		525.1w		
	515.4w	516.9w	516.9w	

In one experiment, Pyrex-filtered photolysis of a matrix containing C₂F₅I/O₂/Ar (1:10:1000) resulted in the detection of bands assigned to carbonyl stretches; the bands increased in intensity on subsequent UV irradiation. Other weak bands were also detected at 983.8 and 965.0 cm⁻¹. Unusually, subsequent UV–vis photolysis produced weak bands at 633.3, 629.6, 608.8 and 581.4 cm⁻¹, which could then be destroyed by Pyrex-filtered photolysis.

C. 1,1,1-Trifluoroiodoethane and Ozone in Argon. The spectra of argon or oxygen matrices containing 1,1,1-trifluoroiodoethane (Table 8) were found to be closely similar to the gas-phase spectra.¹⁶ Ultraviolet photolysis (λ > 240 nm) of CF₃CH₂I isolated in argon for up to 2 h produced no new bands. The spectra of 1,1,1-trifluoroiodoethane (CF₃CH₂I/Ar ~ 1:500) and ozone (O₃/Ar = 1:200 to 1:400) co-deposited in argon have been recorded (Table 8), the bands detected after deposition, subsequent wavelength- and time-dependent photolysis, or warming of the matrices being grouped as follows.

Group 1 bands were formed after co-deposition of the precursors and resemble those detected in the spectra of 1,1,1-trifluoroiodoethane (Table 8) and of ozone¹⁴ isolated separately in argon. The biggest shifts occur for the ν₃ bands of ozone (6.5 cm⁻¹). In the mixed-ozone experiments, bands are assigned to the ν₂ and ν₃ modes and the combination, ν₁ + ν₃ for the six isotopomers. Additionally, some weak bands were detected at 1094.5, 1091.8 and 1090.3 cm⁻¹ which are assigned to the symmetric stretch (ν₁) of the 16–16–18 ozone isotopomer.

Photolysis of the group 1 bands with λ > 650 nm radiation formed the group 2 bands. Visible photolysis (λ > 450 nm) doubled the intensities of these bands, while subsequent UV–vis photolysis (λ > 350 nm) reduced them by 30%; the bands were finally destroyed by Pyrex-filtered irradiation. The group 2 bands include a medium-weak band at 1404.7 cm⁻¹ (a perturbed CH₂ bend), a medium doublet at 1282.1 and 1278.4 cm⁻¹ (CH₂ wags), strong bands at 1257.6 and 1199.2 cm⁻¹ (CF₃ stretches), medium-weak and very weak bands at 732.4 and 727.1 cm⁻¹ (I–O stretches, Table 2 and Figure 6) and weak bands at 554.0 and 543.1 cm⁻¹ (C–I stretches, Table 2).

Group 3 bands were formed after visible photolysis (λ > 410 nm), and destroyed after quartz-filtered irradiation (Table 3).

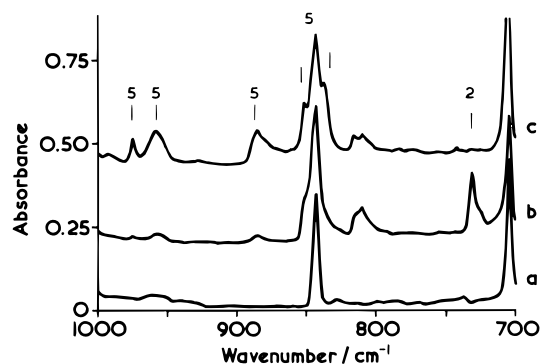


Figure 6. Infrared spectra in the range 1000 and 700 cm^{-1} of a matrix containing $\text{CF}_3\text{CH}_2\text{I}/\text{O}_3/\text{Ar}$ (2:5:1000) after (a) deposition, (b) near-infrared photolysis ($\lambda > 650 \text{ nm}$) and (c) quartz-filtered ($\lambda > 240 \text{ nm}$) photolysis. This shows the growth and loss of the ν_{IO} band of $\text{CF}_3\text{CH}_2\text{IO}$ (group 2), and the growth of some bands of the complex $\text{CF}_3\text{C}(\text{O})\text{H}\cdots\text{HI}$ (group 5).

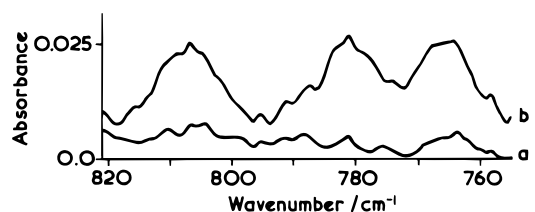


Figure 7. Infrared spectra in the IO_2 stretching region of a matrix containing $\text{CF}_3\text{CH}_2\text{I}/^{16}\text{O}_{3-x}^{18}\text{O}_x/\text{Ar}$ (2:5:1000) after (a) deposition and (b) visible ($\lambda > 410 \text{ nm}$) photolysis, showing bands assigned to iodyl-1,1,1-trifluoroethane, $\text{CF}_3\text{CH}_2\text{IO}_2$ (group 3).

Photolysis with wavelengths intermediate between these two had little effect. In the $^{16}\text{O}_3$ experiments, weak bands were detected at 815.5, 809.4 and 806.9 cm^{-1} , while in the mixed-ozone experiments a number of very weak bands were detected between 811.4 and 752.2 cm^{-1} (Figure 7). These bands are assigned to stretches of the IO_2 unit.

Group 4 bands (very weak) detected after UV-vis photolysis of the matrix at 588.2, 577.7 and 567.4 cm^{-1} (Table 4) are assigned to O-I stretches. A very weak band detected at 3444 cm^{-1} is assigned to an O-H vibration, possibly of HOI.

Group 5 bands are formed after UV-vis ($\lambda > 350 \text{ nm}$) irradiation of the matrix. Pyrex-filtered irradiation doubled the intensities of the bands while quartz-filtered irradiation increased the intensities by approximately 30% for every 30 min cycle. The bands detected are assigned as given in Table 9. Note that a medium band at 1777.8 cm^{-1} and its weak shoulders at 1784.5 and 1765.8 cm^{-1} (Figure 8) (^{18}O at 1748.4, 1743.6 and 1729.1 cm^{-1}) are assigned to carbonyl stretches. In the mixed-ozone experiments, bands were detected that could be assigned to either ^{16}O or ^{18}O isotopomers, confirming that only one oxygen atom is present. No bands were detected that could be attributed to hydrogen iodide.

1,1,1-Trifluoroiodoethane in Oxygen. The spectra of $\text{CF}_3\text{CH}_2\text{I}$ deposited in solid oxygen ($\text{CF}_3\text{CH}_2\text{I}/\text{O}_2 = 1:400$) exhibited bands (Table 8) similar to those detected for the $\text{CF}_3\text{CH}_2\text{I}$ isolated in argon. Quartz-filtered photolysis was required before any product bands (Table 9) were detected; these were assigned, based on their resemblance to the group 5 bands above. In one study, photolysis of the matrix with Pyrex-filtered radiation for 15 h and quartz-filtered radiation for a further 4 h produced a weak band at 3492.3 cm^{-1} (Table 4) assigned to an O-H stretch, probably of the HOI species.

D. 1,1,2,2-Tetrafluoroiodoethane and Ozone in Argon. The spectra of 1,1,2,2-tetrafluoroiodoethane isolated in argon ($\text{CF}_2\text{HCF}_2\text{I}/\text{Ar} = 1:400$) and in solid oxygen ($\text{CF}_2\text{HCF}_2\text{I}/\text{O}_2 =$

TABLE 9: Infrared Bands/ cm^{-1} of the Complex $\text{CF}_3\text{C}(\text{O})\text{H}\cdots\text{HI}$ (Group 5), Detected after Photolysis ($\lambda > 350 \text{ nm}$) of 1,1,1-Trifluoroiodoethane in a Number of Matrices

	O_2	$^{16}\text{O}_3/\text{Ar}$	$^{16}\text{O}_{3-x}^{18}\text{O}_x/\text{Ar}$	$^{18}\text{O}_3/\text{Ar}$	assignment	
1772.5mw		2997.1w	2880.5vw		$\nu_{\text{C-H}}$	
		1784.5w	1783.7w		$\nu_{\text{C=O}}$	
		1777.8m	1778.0mw			
1384.3mw		1765.8vw	1764.7vw			
			1748.0w	1748.4w		
			1743.9mw	1743.6mw		
			1730.8vw	1729.1vw		
			1382.8mw	1377.2mw	$\delta_{\text{i-p C-H}}$	
			1377.4mw			
1215.1s		1301.2ms	1301.2ms	1300.9m	ν_{CF_3}	
		1281.1s	1283.9s			
		1277.3s	1277.0s	1256.6vs		
		1242.1m	1240.4w	1240.4w	$\delta_{\text{CF}_3} + \delta_{\text{FCF}_2}$	
1177.5m		1198.2s	1195.0s	1194.6s	$\delta_{\text{s FCF}_2}$	
		1197.7s				
		1195.3s				
		1177.5m	1170.7s	1173.2ms	1173.9vs	$\nu_{\text{a FCF}_2}$
		1168.3m	1167.4sh, ms	1171.4ms		
			1079.1w	1079.6w	1077.7vw	$\nu_{\text{C-C}} + \rho_{\text{CF}_3}$
		991.8w	974.5w		970.0w	$\delta_{\text{o-o-p CH}}$
		953.3w	958.1mw	958.8w	959.1vw	
			886.7mw			$2\delta_{\text{C-C=O}}^a$
			851.3sh	851.7vw		$\nu_{\text{C-C}}$
707.4mw			843.3m			
			836.6sh	837.0w	833.7w	
			742.3w	695.3w	690.5vw	δ_{CF_3}
				689.0vw		
		598.5vw			δ_{FCF_2}	
		542.7w				
		526.1w				

^a $\delta_{\text{C-C=O}}$ observed elsewhere¹⁷ at 431 cm^{-1} .

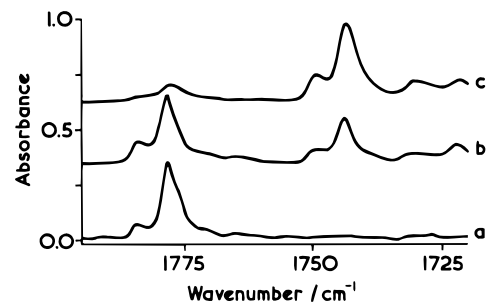


Figure 8. Infrared spectra detected after Pyrex-filtered photolysis of an argon matrix containing $\text{CF}_3\text{CH}_2\text{I}$ and (a) $^{16}\text{O}_3$, (b) $^{16}\text{O}_{3-x}^{18}\text{O}_x$, and (c) $^{18}\text{O}_3$ showing the $\nu_{\text{C=O}}$ bands of the ^{16}O - and ^{18}O -isotopomers of the complex $\text{CF}_3\text{C}(\text{O})\text{H}\cdots\text{HI}$ (group 5).

1:300) were recorded, and the bands assigned (Table 10) using those of other polyfluoroiodoethanes as guides. As with the other species ultraviolet photolysis of $\text{CF}_2\text{HCF}_2\text{I}$ isolated in argon produced no new detectable products. However, the co-deposition of $\text{CF}_2\text{HCF}_2\text{I}$ with ozone in argon ($\text{CF}_2\text{HCF}_2\text{I}/\text{O}_3/\text{Ar} = 1:2:400$) and the subsequent wavelength-dependent photolysis or warming of the matrix resulted in the formation of many new bands.

Group 1 bands, detected after deposition of the precursors, are assigned (Table 10) on the basis of their resemblance to bands of the isolated precursors, $\text{CF}_2\text{HCF}_2\text{I}$ and ozone.¹⁴ The biggest wavenumber shifts occur for the ozone ν_3 bands, which exhibit similar shifts to those detected in the reaction of ozone with the other compounds containing a single iodine atom.¹⁻⁴ In the mixed-ozone ($^{16}\text{O}_{3-x}^{18}\text{O}_x$) experiments six sets of bands were detected for the ν_3 band, indicating that six different isotopomers of ozone were present.

TABLE 10: Infrared Bands/cm⁻¹ of 1,1,2,2-Tetrafluoroiodoethane, CF₂HCF₂I, in a Number of Matrices after Deposition at 14 K

Ar	O ₂	¹⁶ O ₃ /Ar	¹⁸ O ₃ /Ar	assignment
		3039.1w		ν_{C-H}
		2987.7w	2983.0w	
		1413.7w	1414.0w	δ_{H-C-F}
1375vs	1387.9ms	1388.4wm	1388.7ms	
	1374.6s	1374.7s	1375.1vs	
1347.2m	1345.9ms	1346.1wm	1346.3mw	ν_{HCF_2}
	1342.7m			
	1339.2m	1336.3w	1337.1vw	
1242.8w	1243.4wm	1242.6w	1244br, w	ν_{CF_2}
1227.9s	1226.4s	1225.3vs	1226.1s	
	1211.7w		1213.9sh, w	
1186.1w	1185.8w	1198.7w	1198.3vw	ν_{HCF_2}
		1185.9br, w	1186br, w	
1140vs	1167.1w	1163.3mw	1162.3mw	
	1145br, vs	1139.1s	1145br, vs	ν_{CF_2}
1123vs	1131.3vs	1124br, vs	1124br, vs	
	1122.4br, vs	1115.0vs	1114.3vs	
1103.1s	1101.8s	1104.1s	1104.7s	ν_{C-F}
			1103.0sh, s	
	1076.7wm	1078.0w		δ_{H-C-F} or δ_{CF_2}
1049.2s	1058.3wm	1059.3w	1059.2w	
	1050.6vs	1049.9s	1050.4vs	
	942.5vs	940.7vs	940.4vs, br	δ_{HCF_2}
	920.4wm	919.0w		
	883.5w		883.3w	ν_{CF_2I}
	835.5w	840.2w	840.6w	
810.3vs	809.9s	810.1vs	810.9vs	ν_{C-C}
			680.3vw	ν_{C-I}
			675.8vw	
658.1m	656.3m	658.7m	658.2m	δ_{HCF_2}
656.4m		656.6m	656.3sh, m	
618.7m	618.7m	618.9s	618.8m	
592.9s	586.3s		593.9vs	
	550.1mw		584.5s	

Near-infrared photolysis ($\lambda > 650$ nm) of matrices containing group 1 bands produced the group 2 bands. Visible photolysis ($\lambda > 410$ nm) increased the band intensities by 20%, but UV-vis ($\lambda > 350$ nm) irradiation destroyed them. These bands include ones at 1187.4 cm⁻¹ (perturbed ν_{C-F}), 908.4 and 903.3 cm⁻¹ (ν_{CF_2I}), 562.8 cm⁻¹ (δ_{CF_2}), 534.4 cm⁻¹ (ν_{C-I} , Table 2), and 739.5–722.3 cm⁻¹ (ν_{I-O} , Table 2), based on the ¹⁸O-shifts of 36.2 and 41.7 cm⁻¹ between the ¹⁶O bands at 727.6 and 722.3 cm⁻¹ and the ¹⁸O bands at 691.4 and 680.6 cm⁻¹.

Group 5 bands were formed after UV-vis irradiation; Pyrex- and quartz-filtered irradiation doubling the intensities after each photolysis cycle. The bands are assigned in Table 11: note that the strong bands at 1942.0, 1938.5 (¹⁸O at 1906.8 cm⁻¹) and 1909.0 cm⁻¹ (¹⁸O at 1874.8 cm⁻¹) and medium-weak bands at 1888.3 and 1867.3 cm⁻¹ (¹⁸O at 1861.7 cm⁻¹) are assigned to carbonyl stretches (Figure 9), based on the ¹⁸O-shifts of ~ 35 cm⁻¹.

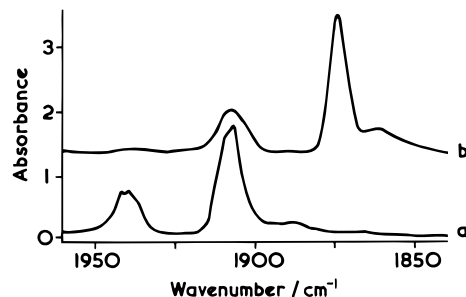
Warming the matrix caused some bands to decrease in intensities while others, assigned to the same mode, are unaffected or increased in intensity slightly. The largest effect was detected for the carbonyl stretch for which warming reduced the intensities of the bands between 1942.0 and 1909.0 cm⁻¹ by ~ 20%. Bands at 764.3 and 625.4 cm⁻¹ were also reduced slightly in intensities.

E. 1,1,1,2-Tetrafluoroiodoethane and Ozone in Argon. The spectra of argon matrices of 1,1,1,2-tetrafluoroiodoethane (CF₃CFHI/Ar = 1:600) were recorded and the bands assigned (Table 12) using the previously studied polyfluoroiodoalkanes as guides. Ultraviolet photolysis of CF₃CFHI isolated in argon produced no new detectable bands.

The spectra recorded after co-deposition of 1,1,1,2-tetrafluoroiodoethane (CF₃CFHI/Ar = 1:200) and ozone (O₃/Ar =

TABLE 11: Infrared Bands/cm⁻¹ Assigned to CF₂HC(O)F...IF (Group 5), Detected after 350 nm Irradiation of an Argon Matrix Containing the Precursors 1,1,2,2-Tetrafluoroiodoethane and Ozone

¹⁶ O ₃ /Ar	¹⁸ O ₃ /Ar	assignment
1942.0s	1906.8m	$\nu_{C=O}$
1938.5s		
1909.0vs	1874.8s	
1888.3mw		
1867.3mw	1861.7w	
1329.1m	1329.3m	$\nu_a HCF_2$
1270.2mw	1269.9sh, mw	$\nu_s HCF_2$
1265.3mw	1265.5sh, mw	
1258.3m	1249.9m	
1250.5s	1245.6m	
1246.5ms		
	1178.4mw	$\delta_{O-C-F} + \omega_{i-ph}$
	1167.1w	
1079.0ms	1078.8m	ν_{C-F}
1064.2m	1063.9w, br	
969.1m		δ_{H-C-F}
856.8mw		ν_{C-C}
849.7mw		
770.9m	767.1mw	δ_{O-C-F}
764.3mw	760.0mw	
633.0mw	632.4w	δ_{HCF_2}
625.4mw	625.5w	
	606.3vw	$\nu_s I-F$

**Figure 9.** Infrared spectra after Pyrex-filtered irradiation of an argon matrix containing CF₂HCF₂I and (a) ¹⁶O₃ and (b) ¹⁸O₃, showing the $\nu_{C=O}$ bands of the ¹⁶O- and ¹⁸O-isotopomers of the complex CF₂HC(O)F...IF (group 5).

1:400) in argon exhibited a number of bands. Subsequent wavelength- and time-dependent photolysis and warming of the matrices produced various new bands.

Group 1 bands were detected after co-deposition of 1,1,1,2-tetrafluoroiodoethane and ozone in argon, and they resemble those assigned to the precursors, CF₃CFHI (Table 12) and ozone¹⁴ except for minor perturbations. The bands assigned to ozone exhibited the largest perturbations, and in the mixed-ozone experiments bands were detected for the six isotopomers of ozone. Again, like the other ozone complexes detected in these studies, efficient photolysis occurs with near-infrared radiation ($\lambda > 650$ nm) to form the group 2 bands.

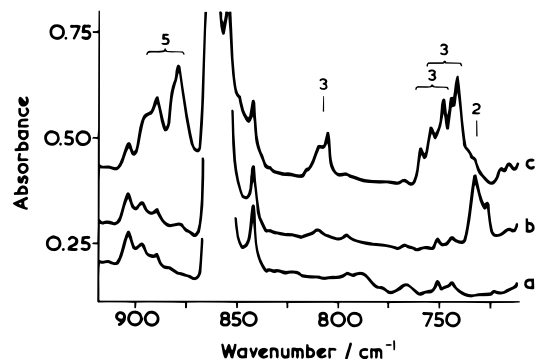
Photolysis at $\lambda > 550$ nm and $\lambda > 410$ nm increased the band intensities, while shorter wavelength ($\lambda > 350$ nm) irradiation destroyed the bands, which include ones at 1262.7 cm⁻¹ (ν_{C-F}), 810.7 cm⁻¹ (ν_{C-C}), 732.0 and 726.0 cm⁻¹ (ν_{I-O} , Table 2 and Figure 10), this being confirmed by the ¹⁸O-shift of 37.4 cm⁻¹ for the ¹⁶O band at 732.0 cm⁻¹, and 549.6 and 547.7 cm⁻¹ (ν_{C-I} , Table 2).

Group 3 bands were formed after UV-vis ($\lambda > 350$ nm) photolysis of the matrix, the low intensities preventing any changes from being detected after subsequent Pyrex- and quartz-filtered photolysis. They include (Table 3 and Figure 10) bands at 815.8, 810.2 and 805.1 cm⁻¹ (ν_{I-O_2}).

Group 5 bands were formed after UV-vis photolysis, and increased in intensity by ~ 40% and 20% after subsequent

TABLE 12: Infrared Bands/cm⁻¹ of 1,1,1,2-Tetrafluoroiodoethane in a Number of Matrices after Deposition at 14 K

Ar	¹⁶ O ₃ /Ar	¹⁶ O _{3-x} ¹⁸ O _x /Ar	¹⁸ O ₃ /Ar	assignment
3013.2w	3015.8w		3014.1w	ν_{C-H}
			2879w	
1430.5mw	1430.2mw		1430.7w	δ_{H-C-F}
1368.3sh, s	1360.3vs	1368.4m	1368.3s	ν_{CF_3}
1362.6vs	1353.9s	1362.0s	1361.9vs	
1353.5s			1353.7sh, s	
1294.7w	1286.1ms	1287.5s	1286.7vs	
1286.8s	1273.0s	1277.2vs	1275br, vs	
1274.9vs	1263.1w	1274.9vs	1262.3sh, w	
1262.5m		1262.3m		
1250.6m	1249.6mw	1249.9w	1249.9mw	$\nu_a CF_3$
1249sh, m		1244.8w		
1244.0mw	1244.2w	1236.0ms		
1235.0vs	1234.2vs	1206.1sh, m	1235.6s	
1197.9br, vs	1195.0vs	1197.3vs	1196br, vs	ν_{C-F}
1164.3mw	1163.4w	1163.9w	1164.0w	$\nu_s CF_3$
1153.3mw	1152.2w	1153.5w	1153.5w	
		1132.9sh, m	1132.3sh, s	ν_{H-C-F}
1126.2br, vs	1122.4vs	1125.9vs	1124.0vs	
1105.7mw	1104.8w	1105.3w	1105.7s	
1093.6ms		1093.6mw	1093.5m	ν_{C-F}
1092.1sh, ms	1092.2mw	1091.5mw	1086.5m	
1086.6m	1086.8w	1087.3w	1075.8s	δ_{H-C-F}
1077.1vs	1073.7vs	1076.1s	1069.8sh, m	
1062.8s	1062.9s	1061.8mw	1063.3m	
862.4vs	861.8vs	863.4mw	863.2s	ν_{C-C}
854.4m	854.6m	854.9w	854.8mw	
683.7m	684.2m	684.2m	684.3m	ν_{C-I}
	658.2w	657.7w	652.9w	δ_{CF_3}
567.2w	566.9s	567.1m	567.2m	
526.6w				
522.2mw	522.4m	522.1mw	521.9mw	
516.5mw	516.4m	516.5mw	516.4wm	

**Figure 10.** Infrared spectra in the region 900 and 725 cm⁻¹ of a matrix containing CF₃CFHI/¹⁶O_{3-x}¹⁸O_x/Ar (2:1:400) after (a) deposition, (b) visible ($\lambda > 410$ nm) photolysis and (c) Pyrex-filtered photolysis, showing the growth and loss of the ν_{10} band of CF₃CFHIO (group 2), growth of the ν_{10_2} bands of CF₃CFHIO₂ (group 3), and growth of some bands of the CF₃C(O)F \cdots HI complex (group 5).

Pyrex- and quartz-filtered photolysis, respectively. The bands detected (Table 13) include ones between 1894.2 and 1792.0 cm⁻¹ ($\nu_{C=O}$) (Figure 11, ¹⁸O-shift of 35.5 cm⁻¹), 1336.3 cm⁻¹ (¹⁸O-shift of 2.8 cm⁻¹) (ν_{CF_3}), 1286.9 and 1247.3 cm⁻¹ (ν_{CF_3}), 1092.6 and 1087.2 cm⁻¹ (ν_{C-F}), 890.9 and 879.5 cm⁻¹ (ν_{C-C} , Figure 10), 690.5 cm⁻¹ (δ_{CF_3}) and 603.6 cm⁻¹ can be assigned to either a vibration described by the mixing of an OCF' bend and a CF₃ bend, or to the I-F stretch.

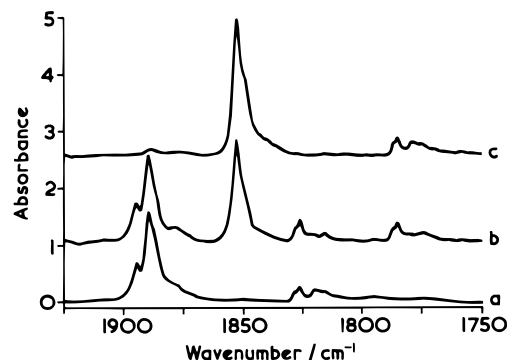
Discussion

The various bands reported above for each experiment, are grouped below according to the chemical species to which they refer and their photolytic and thermal behavior.

Precursor \cdots Ozone Complex. These bands (group 1) are detected after co-deposition of each of the five iodine-containing

TABLE 13: Infrared Bands/cm⁻¹ of the Group 5 Carbonyl Complexes, CF₃C(O)F \cdots HI and CF₃C(O)H \cdots IF, Formed after UV-Vis ($\lambda > 350$ nm) Irradiation of an Argon Matrix Containing 1,1,1,2-Tetrafluoroiodoethane and Ozone

¹⁶ O ₃ /Ar	¹⁶ O _{3-x} ¹⁸ O _x /Ar	¹⁸ O ₃ /Ar	assignment
1894.2m	1894.8w		$\nu_{C=O} CF_3C(O)F$
1888.5ms	1889.3m		
1877.2w	1877.6w		
	1853.2m	1853.0ms	
1826.0w	1826.2w		$\nu_{C=O} CF_3C(O)H$
1815.5w	1815.2w		
1792.0w	1785.3mw	1785.3mw	
	1779.1vw	1778.7w	
	1774.8w	1774.6w	
1409.2w		1408.6mw	$2\delta_{CF_3} ?$
1336.3w	1334.4mw	1333.5mw	ν_{CF_3}
1286.9s			ν_{FCF_2}
		1259.4sh, w	
1247.3m	1246.3m	1246.9m	
1185.1s	1185.0sh, w	1184.1ms	$\delta_{O-C-F} + \omega_{i-ph} ?$
1177.4sh, w	1177.9sh, w	1178.3mw, sh	
1092.6mw	1091.7m	1093.5mw	ν_{C-F}
1087.2w		1091.5mw	
		1089.2s	
	1069.2sh, w	1069.5ms	$\delta_{CF_3} + \rho_{i-ph} ?$
1061.5s	1064.2w		
	1053.8w	1054.1w	
	890.9w	878.4w	ν_{C-C}
	879.5w		
690.5mw	691.4sh, w		δ_{CF_3}
676.1w			$\omega_{i-ph} + \omega_{o-ph} ?$
635.2vw			
603.6br, w		592.5w	$\delta_{O-C-F}, \delta_{FCF_2}$ or $\nu_{s I-F}$
		582.9w	
	526.4vw		δ_{F-C-F}

**Figure 11.** Infrared spectra recorded after Pyrex-filtered irradiation of argon matrices containing CF₃CFHI and (a) ¹⁶O₃, (b) ¹⁶O_{3-x}¹⁸O_x and (c) ¹⁸O₃, showing the $\nu_{C=O}$ bands of the ¹⁶O- and ¹⁸O-isotopomers of the complexes CF₃C(O)F \cdots HI and CF₃C(O)H \cdots IF (group 5).

species and ozone in argon matrices and resemble the bands detected for the precursors isolated separately in argon (Tables 1, 6, 8, 10, and 12), except for small perturbations. The bands assigned to ozone exhibit the largest wavenumber shifts, comparable to those for precursor \cdots ozone complexes discussed elsewhere.²⁻⁴ In each case, the complex perturbs the photochemistry by allowing ozone to be dissociated after near-infrared irradiation ($\lambda > 800$ nm for 2-iodopropane and $\lambda > 650$ nm for the polyfluoroiodoethanes); this photodissociation occurs via a charge-transfer type mechanism, similar to that reported previously⁴ in which an oxygen atom is transferred from ozone to the iodine atom of the iodinated alkane to form the iodoso-species. The difference in threshold wavelength required to initiate a reaction is probably due to a difference in ionization energies between 2-iodopropane and the polyfluoroiodoethanes.

Iodoso-Species. Group 2 bands are formed after near-infrared photolysis of matrices each containing one of the halocarbons and ozone, and are finally destroyed by UV-vis

($\lambda > 350$ nm) or Pyrex-filtered irradiation. In each experiment the growth of these bands appeared to occur at the expense of the group 1 bands, indicating a stepwise mechanism. Possibly the most diagnostic bands detected for this group, despite their weakness, are assigned to I–O and C–I stretches (Table 2). The wavenumbers are close to the ν_{10} values for other hydrated and fluorinated iodoso-species (between ca. 714 and 740 cm^{-1}) detected previously.^{2–4} Also the ^{18}O -shifts are very close to that predicted for I–O, and the detection of bands for either the ^{16}O or ^{18}O isotopomer suggests the presence of a single oxygen atom in this species. Thus the presence of an iodoso-species (Z–IO) is indicated in each case.

Several similar iodoso-species (ClIO ,¹ CH_3IO ,² CF_3IO ,³ $\text{C}_2\text{H}_5\text{IO}$,⁴ and HIO^{18}) have been reported to have the Z–IO structure. The addition of methyl groups shifts ν_{10} to lower wavenumbers, e.g. iodosomethane,² $\text{H}_3\text{C–IO}$, (723.7 cm^{-1}) and 2-iodosopropane, $(\text{CH}_3)_2\text{CH–IO}$, (714.5 cm^{-1}). This trend is caused by the methyl groups donating electron density into the (p–p) π^* orbital of the I–O bond. Trifluoromethyl groups (CF_3) on the other hand, have the reverse effect on ν_{10} on account of their electron withdrawing capabilities; thus the ν_{10} values of iodosotrifluoromethane, $\text{CF}_3\text{–IO}$,³ (732.7 cm^{-1}) and iodosopentafluoroethane, $\text{C}_2\text{F}_5\text{–IO}$, (738.7 cm^{-1}) are above those of their alkyl counterparts. The remaining species, $\text{CF}_3\text{CH}_2\text{–IO}$ (732.4 and 727.1 cm^{-1}), $\text{CF}_2\text{HCF}_2\text{–IO}$ (727.6 and 722.3 cm^{-1}) and $\text{CF}_3\text{CFH–IO}$ (732.0 and 726.0 cm^{-1}) can also be compared with those above.

Iodol-Species. The iodol-species bands (group 3) were formed after visible ($\lambda > 410$ nm) and UV–vis ($\lambda > 350$ nm) photolysis of matrices, each containing ozone and one of the iodine-containing precursors. However, any bands attributable to iodol-species formed during the 1,1,2,2-tetrafluoroiodoethane/ozone experiment were too weak to be detected. Destruction of such bands after subsequent Pyrex- and quartz-filtered photolysis was only observed in a few cases, while in others, the low intensities prevented any changes from being detected. This group of bands is assigned to various IO_2 stretches (Table 3). Bands in the 800–830 cm^{-1} region detected in the $^{16}\text{O}_3$ experiments, and assigned to the anti-symmetric I^{16}O_2 stretch, are similar to those attributed to iodylethane (837.2–825.4 cm^{-1}) and iodyltrifluoromethane (799 cm^{-1}). In the experiments involving $^{16}\text{O}_3$ with $\text{C}_2\text{F}_5\text{I}$ or $\text{CF}_3\text{CH}_2\text{I}$, no bands assigned to the symmetric stretch were detected due to the low absorbance and, in the former case, also to near coincidence with the OCF' bend of tetrafluoroethanal at 760–770 cm^{-1} . In the mixed-ozone experiments, the bands were assigned using the criteria employed elsewhere⁴ (i.e. ^{18}O -shift ~ 40 cm^{-1} ; $\nu_a\text{IO}_2 - \nu_s\text{IO}_2 \sim 34$ cm^{-1} ; ν_{10} (of Z–IO) $- \nu_s\text{IO}_2$ (of Z– IO_2) ~ 60 –80 cm^{-1}). Additionally, the antisymmetric and symmetric stretches of the various IO_2 isotopomer units support the conclusion that this unit contains two oxygen atoms. Thus the presence of these IO_2 units suggests the existence of the iodol-species (Z– IO_2) which are believed to be formed via a reaction of the precursor (Z–I) with an excited oxygen molecule, or possibly via a reaction of the related iodoso-species (Z–IO) with an oxygen atom.

Hypoiodo-Species. These bands (group 4) were formed after UV–vis ($\lambda > 350$ nm) photolysis of argon matrices containing ozone and either $(\text{CH}_3)_2\text{CHI}$, $\text{C}_2\text{F}_5\text{I}$ or $\text{CF}_3\text{CH}_2\text{I}$, and are assigned to either O–H, C–O or O–I stretches (Table 4), depending on the precursor involved. No bands of this type were detected following the reaction of ozone with either of the precursors $\text{CF}_2\text{HCF}_2\text{I}$ or CF_3CFHI , again due to the low intensities, but the subsequent formation of photoproducts (group 5) confirms that the same interconversion route is followed by the other

precursors. Where possible to detect, the formation of the group 4 hypoiodo-type bands (Z–OI) coincided with the loss of the iodoso-species bands (group 2); the group 4 bands were destroyed by Pyrex-filtered irradiation.

In the matrix isolation experiment of 2-iodopropane and ozone, bands are assigned to an O–H and an O–I stretch and thus to hydrogen hypoiodide, HOI. The ν_{OI} band could possibly be attributed to the O–I vibration of the C–O–I unit, except that no other bands were detected which could be attributed to this hypoiodo-species. However, given the species reported previously⁴ and for the other precursors in this work, it seems likely that 2-hypoiodopropane might be present. The detection of HOI here agrees with the gas-phase results of Leone¹⁹ et al. Using pentafluoroiodoethane as the precursor, bands detected are assigned to C–O and O–I stretches. The ν_{OI} bands of HOI and $\text{C}_2\text{F}_5\text{OI}$ are separated by ~ 9 cm^{-1} , and thus it seems possible that the bands detected in this experiment could be attributed to ν_{OI} of the fluoro-analogues, $\text{CF}_3\text{CF}_2\text{OI}$ and FOI. The FOI species would be formed in much the same manner as is HOI in the iodoethane/ozone experiments, i.e., via a five-membered ring intermediate. Unfortunately, no O–F stretching bands were detected (the ν_{OF} bands of the triatomics $\text{FON}^{20–22}$ and $\text{FO}_2^{23,24}$ occur at 492 and 584 cm^{-1} , respectively). Using the 1,1,1-trifluoroiodoethane precursor, bands were detected at 588.2, 577.7, and 567.4 cm^{-1} , which supports their assignment to O–I stretches, possibly of $\text{CF}_3\text{CH}_2\text{OI}$, HOI or FOI. The weak band at 3444 cm^{-1} (3492.3 cm^{-1} in the oxygen matrix) tentatively assigned to the O–H vibration suggests the presence of HOI. The presence of FOI would be expected if the five-membered ring intermediate mechanism were operating, but again no ν_{OF} bands were detected. The presence of HOI is accounted for by the reaction of HI (from $\text{CF}_3\text{CH}_2\text{I}$) with oxygen atoms,¹⁸ and this mechanism almost certainly operates for the oxygen matrix experiment in which over 19 h of photolysis was employed. This observation might also account for the disparity whereby HOI was detected in the matrix reactions of iodomethane^{25,26} and molecular oxygen (during which long periods of ultraviolet photolysis were required) but not in the matrix² and gas-phase¹⁹ experiments using ozone to produce oxygen atoms. The lack of detection of FOI, and the tentative evidence for HI would at first tend to suggest that a five-membered ring intermediate was not being formed; however, as will be discussed later, it is thought that the intermediate rapidly rotates around the α -carbon to give the observed products.

Carbonyl Complexes. These bands were first detected after UV–vis photolysis ($\lambda > 350$ nm) of the matrices and they increased in intensity after subsequent Pyrex- and quartz-filtered irradiation. Like the hypoiodo-species bands, the formation of this group of bands appeared to be at the expense of the iodoso-species bands. However, unlike the hypoiodo-type bands, these bands continued to grow after Pyrex- and quartz-filtered photolysis, providing further support for a stepwise reaction in which photolysis converts iodoso- into hypoiodo-species and then to carbonyl-species. These bands (group 5) are attributable to several carbonyl \cdots Lewis acid complexes, which were the final species detected. In all cases the carbonyl stretching bands are the most diagnostic. The various carbonyl \cdots Lewis acid complexes are discussed below.

(i) $(\text{CH}_3)_2\text{CO}\cdots\text{HI}$. Bands attributable to this species were detected after photolysis of ozone and 2-iodopropane (Table 5). The most diagnostic bands are those assigned to the carbonyl stretch, $\nu_{\text{C=O}}$ and, based on the similarity of the band wavenumbers to those previously noted, these group 5 bands have been attributed to acetone.^{27–29} By examining the wavenumber

TABLE 14: Infrared Bands/cm⁻¹ Assigned to the Carbonyl Stretch of the Polyfluoroethanals, CX₃C(O)X (X = H or F), Perturbed by Either HI or IF

complex	precursor	$\nu_{C=^{16}O}$	$\nu_{isolated} - \nu_{complexed}^a$
CF ₃ C(O)F...IF	C ₂ F ₅ I	1938.4ms	-39.4
		1936.4ms	-37.4
		1933.9ms	-34.9
		1909.9ms	-10.9
		1907.7s	-8.7
		1905.9s	-6.9
CF ₂ HC(O)F...IF	CF ₂ HCF ₂ I	1901.2sh, s	-2.2
		1886.3mw	12.7
		1942.0s	-43.0
		1938.5s	-39.5
		1909.0vs	-10.0
CF ₃ C(O)F...HI	CF ₃ CHFI	1888.3mw	10.7
		1867.3mw	31.7
		1894.2m	4.8
CF ₃ C(O)H...IF	CF ₃ CHFI	1888.5ms	10.5
		1877.2w	21.8
		1826.0w	-38.0
CF ₃ C(O)H...HI	CF ₃ CH ₂ I	1815.5w	-27.5
		1792.0w	-4.0
		1784.5w	3.5
CF ₃ C(O)H...HI	CF ₃ CH ₂ I	1777.8m	10.2
		1765.8vw	22.2

^a $\nu_{isolated}$ of CF₃C(O)F³⁴ = 1899 cm⁻¹, of CF₃C(O)H = 1788 cm⁻¹, for CF₂HC(O)F use $\nu_{isolated}$ = 1899 cm⁻¹ (same as CF₃C(O)F), +ve = shift to lower wavenumber, -ve = shift to higher wavenumber.

shift relative to that of isolated acetone,²⁹ it is possible to attribute these bands to three acetone complexes in argon. The medium-weak band at 1723.2 cm⁻¹ is the $\nu_{C=O}$ band of acetone isolated in argon. The other carbonyl bands are assigned to two acetone-hydrogen iodide complexes; a medium band at 1719.2 cm⁻¹ is attributed to a molecular-pair complex, while medium-to-weak bands at 1712.9, 1706.9 and 1700.3 cm⁻¹, are attributed to a complex involving a hydrogen bond between acetone and HI. Although no hydrogen iodide was detected in this study, the bands can be compared to those in which acetone and HI were deposited separately and resulted in the formation of similar complexes.²⁹ Matrices containing various initial 2-iodopropane/ozone ratios produced no additional bands, indicating that a 1:1 complex between HI and acetone is formed from oxygen-atom addition to 2-iodopropane.

(ii) CX₃C(O)X...HI or ...IF (Where X = F or H). The reaction of oxygen atoms with the four polyfluoroethanes has produced a number of polyfluorocarbonyls complexed with either HI or IF (Table 14).

The majority of group 5 bands detected for the pentafluoroiodoethane precursor (Table 7), resemble those previously reported for CF₃C(O)F in the gas phase³⁰⁻³³ and in an argon matrix,³⁴ while the band at 596.5 cm⁻¹ resembles those assigned to IF, reported previously in the gas phase,³⁵ isolated in an argon matrix,³⁶ and in the complex COF₂...IF.³ Based on this spectral evidence these group 5 bands were attributed to the complex CF₃C(O)F...IF. On warming to ca. 30 K, the intensity of the carbonyl band at 1886.8 cm⁻¹ increased at the expense of those centered around 1936 cm⁻¹. Thus bands that increased in intensity or remained unchanged after the sample was warmed have been assigned to a more thermally stable arrangement, involving a head-to-tail dipole-dipole interaction between the O and I atoms of the CF₃C(O)F and IF, while bands that reduced in intensity are assigned to a complex involving a molecular-pair type complex with the C=O and IF bonds parallel to each other.

In matrices containing ozone and 1,1,1-trifluoroiodoethane, the group 5 bands detected after photolysis (Table 9) are in good agreement with those reported in the gas-phase spectra of CF₃C(O)H.¹⁷ No bands were detected for hydrogen iodide, but due to its low infrared absorbance this is not entirely unexpected, and the detection of HOI (group 4 bands) provides support for the presence of hydrogen iodide. Therefore this group of bands is attributed to the complex CF₃C(O)H...HI.

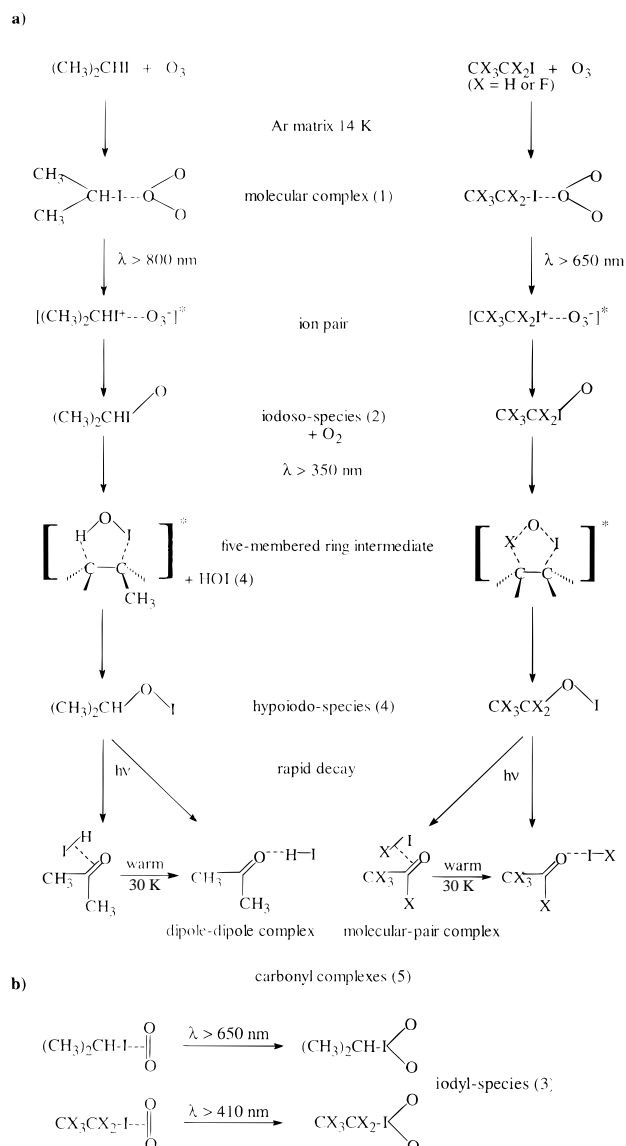
Employing 1,1,2,2-tetrafluoroiodoethane as an initial precursor, the group 5 bands (Table 11) are assigned using CF₃C(O)F³⁴ and CF₃C(O)H¹⁷ as guides, i.e., the detection of bands attributable to either the -COH or -COF unit should be diagnostic of the carbonyl species present. The bands between 1942.0 and 1867.3 cm⁻¹ (¹⁸O between 1906.8 and 1861.7 cm⁻¹) are assigned to the $\nu_{C=O}$ of CF₃C(O)F³⁴ (1899 cm⁻¹) rather than to that of CF₃C(O)H¹⁷ (1788 cm⁻¹). In addition, the bands at 1079.0 and 1064.2 cm⁻¹ are assigned to the ν_{C-F} and those at 770.9 and 764.3 cm⁻¹ to δ_{OCF} . No bands were detected that could be assigned to any C-H' bends. By comparison of the bands detected with those of carbonyls having a -COF unit, it is clear that the species must be CF₂HC(O)F, 1,1,2-trifluoroethanal. In addition, a very weak band at 606.3 cm⁻¹, detected in the ¹⁸O₃ experiments, provides tentative evidence for the presence of IF, and for the complex CF₂HC(O)F...IF. The wavenumber shifts of the $\nu_{C=O}$ bands are in good agreement with those of other carbonyl...IF complexes. Again, warming the matrix indicated that the complex existed in two geometries distinguished by their thermal stabilities.

The final precursor in this study, 1,1,1,2-tetrafluoroiodoethane, also produced group 5 bands after photolysis with ozone in an argon matrix. The bands detected (Table 13) are attributed, by comparison with those of CF₃C(O)F³⁴ and CF₃C(O)H,¹⁷ to the complexes CF₃C(O)F...HI and CF₃C(O)H...IF. The most diagnostic bands for these complexes are those assigned to the $\nu_{C=O}$ stretch (Figure 11).

Examination of the carbonyl bands of these carbonyl...Lewis acid complexes provides us with two pieces of information. First the wavenumber enables us to distinguish the environment of the carbonyl band, i.e., carbonyls having either -COH or -COF units; positive identification of the final products helps to distinguish between possible competing mechanisms for their production. Second, the wavenumber shift ($\Delta = \nu_{isolated} - \nu_{complexed}$) of the complexed bands from those of the isolated carbonyl, can be used to distinguish between the complexes perturbed by IF or HI and, more importantly, to supply information as to the geometry and nature of the bonding between the carbonyl and the Lewis acid.

For cases in which HI is the Lewis acid, the $\nu_{C=O}$ bands are shifted to lower wavenumbers (Table 14), e.g. those of CF₃C(O)F...HI are shifted by 4.8, 10.5 and 21.8 cm⁻¹ and those of CF₃C(O)H...HI by 3.5, 10.2 and 22.2 cm⁻¹. For these complexes, the least shifted bands ($\Delta < 5$ cm⁻¹) are assigned to a weak complex in which the HI has very little effect on the carbonyl. The medium shifted bands ($\Delta \sim 10$ cm⁻¹) are attributed to a molecular-pair complex between HI and the carbonyl. Finally, the most perturbed bands ($\Delta > 20$ cm⁻¹) are attributed to a complex involving a hydrogen bond between the hydrogen atom of hydrogen iodide and the oxygen atom of the carbonyl bond. For further comparison these wavenumber shifts can be compared to those detected previously for the $\nu_{C=O}$ bands of the carbonyl...HI complexes: COH₂...HI ($\Delta\nu = 6.1$ and 12.4 cm⁻¹)² (16 cm⁻¹),³⁷ CH₃C(O)H...HI (9, 16.3, 19 and 22.6 cm⁻¹)⁴ and (CH₃)₂CO (8, 12 and 17 cm⁻¹)²⁹ (2, 10.3, 16.3 and 22.9 cm⁻¹, this work).

SCHEME 1



For the complexes perturbed by IF, the $\nu_{C=O}$ bands are shifted both to higher and to lower wavenumbers (Table 14); thus, for the complex $CF_3C(O)F \cdots IF$, bands are blue-shifted by 39.4, 37.4, 34.9, 10.9, 8.7, 6.9 and 2.2 cm^{-1} and red-shifted by 12.7 cm^{-1} , while for $CF_2HC(O)F \cdots IF$, bands are blue-shifted by 43.0, 39.5 and 10.0 cm^{-1} and red-shifted by 10.7 and 31.7 cm^{-1} . For $CF_3C(O)H \cdots IF$ the bands are blue-shifted by 38.0, 27.5 and 4.0 cm^{-1} . First, the blue-shifted bands can be split into three groups: (i) Δ between 30 and 40 cm^{-1} , (ii) $\Delta \sim 10$ cm^{-1} and (iii) $\Delta < 5$ cm^{-1} . The red-shifted bands have shifts of c. 10 cm^{-1} . Thus for the carbonyl $\cdots IF$ complexes there are three types of complex: two blue-shifted and one red-shifted (the bands blue-shifted by less than 5 cm^{-1} involve only a very weak complex). The bands with the largest blue-shift are assigned to a complex with the I-F bond parallel with the carbonyl bond (molecular-pair complex). Finally, the red-shifted bands are assigned to a complex involving the head-to-tail, dipole-dipole interaction between the iodine of IF and the oxygen atom of the carbonyl. These red shifts, and especially the band shifted by 31.7 cm^{-1} detected for $CF_2HC(O)F \cdots IF$, indicate that the IF complexes are at least as strong as their hydrogen iodide counterparts.

Photochemical Interconversion. The photochemical pathway (Scheme 1a) is similar to that proposed for the analogous

iodoethane reaction.⁴ The first species detected after deposition is a weak complex between ozone and one of the iodine-containing precursors, e.g. $(CH_3)_2CHI \cdots O_3$ and $C_2X_5I \cdots O_3$ ($X = H$ or F). The formation of such a complex alters the photochemistry of ozone sufficiently for effective transfer of an oxygen atom to the iodine substituent after near-infrared photolysis ($\lambda > 800$ nm and $\lambda > 650$ nm). This transfer occurs via a charge-transfer type mechanism, forming an iodoso-species ($(CH_3)_2CH-I-O$ or C_2X_5-I-O) having a C-I-O linkage. Subsequent UV-vis ($\lambda > 350$ nm) irradiation destroys the iodoso-species to form the group 4 hypoiodo-species ($Z-OI$). However, appropriate bands were not detected in all of these matrix experiments due to low intensities. Further Pyrex- ($\lambda > 290$ nm) or quartz- ($\lambda > 240$ nm) filtered photolysis forms easily identifiable carbonyl complexes (group 5). The mechanism of interconversion between these species is of interest since, in the gas-phase reaction of ozone with iodoethane,⁵ and other iodoalkanes,³⁸ a five-membered ring intermediate was proposed which gave rise to HOI. The aim in these studies was to detect bands that could provide direct evidence for the presence of a five-membered ring intermediate and hence species such as FOI and HOI as well as $(CH_3)_2CHOI$ and C_2X_5OI . The main doubt centered on whether the C-I-O bond rearranged to form a five-membered ring, or whether the rearrangement was centered on the carbon atom containing the C-I bond. In fact the final rearrangement is believed to be a combination of both, in which the C-I-O bond rotates to form a weak five-membered ring intermediate; if the β -carbon has H atoms attached (as with iodoethane and 2-iodopropane) then HOI is detected, whereas if the β -carbon has F atoms then FOI is not detected due to the stronger C-F bond. In low-temperature matrices the five-membered ring intermediate rotates further to bring the O atom close to the C atom (on which the I atom is attached) forming a new C-O bond, hence the hypoiodo-species, $Z-OI$. These hypoiodo-species rapidly decay forming a C=O bond and the I atom abstracts either an H or F atom (depending on the precursor) from the α -carbon to form HI or IF, respectively, and hence the carbonyl $\cdots XI$ complex ($X = H$ or F). In the gas-phase reaction of iodoethane and ozone, however, the five-membered ring dissociates into HOI and ethene. Fortunately, the detection of the final carbonyl complexes proved very useful since this helped us to determine the mechanism without having to detect either the five-membered ring intermediate or, in some instances, the hypoiodo-species. Annealing the matrix, in some experiments, enabled two geometric arrangements of the final complexes to be identified.

In the solid oxygen matrices, similar carbonyl \cdots Lewis acid complexes were detected, which suggests that the oxygen atoms produced are able to insert into the C-I bond in the same manner as those produced in the ozone experiments. The lack of intermediate products is accounted for by the shorter wavelength radiation required to generate oxygen atoms, which effectively destroys any intermediates which form.

A final group of species (Scheme 1b) was detected after photolysis with visible radiation; these species resemble those detected elsewhere⁴ and are considered to be the iodyl-species, $(CH_3)_2CHIO_2$ and $C_2X_5IO_2$. The low yields in these experiments were matched by the low yields reported for the reaction between ozone and trifluoroiodomethane.³

Conclusions

The reactions between ozone and 2-iodopropane or the polyfluoroiodoethanes have produced many intermediates with various iodine-oxygen bonds as well as many new carbonyl complexes. The photochemical reaction path (Scheme 1) has

been shown to account for the species detected and to support the mechanism previously proposed as well as the results of the gas-phase¹⁹ reactions.

Acknowledgment. J.R.D. and L.J.F. thank the EPSRC for financial support.

References and Notes

- (1) Hawkins, M.; Andrews, L.; Downs, A. J.; Drury, D. J. *J. Am. Chem. Soc.* **1984**, *106*, 3076–3082.
- (2) Hawkins, M.; Andrews, L. *Inorg. Chem.* **1985**, *24*, 3285–3290.
- (3) Andrews, L.; Hawkins, M.; Withnall, R. *Inorg. Chem.* **1985**, *24*, 4234–4239.
- (4) Clark, R. J. H.; Dann, J. R. *J. Phys. Chem.* **1996**, *100*, 532–538.
- (5) Leone, S. R.; Klaassen, J. J.; Lindner, J. *Abs. Pap. Am. Chem. Soc.* **1995**, *210*, 171–Phys.
- (6) Francis, W. C.; Haszeldine, R. N. *J. Chem. Soc.* **1955**, 2151–2163.
- (7) Clemitshaw, K. C.; Sodeau, J. R. *J. Phys. Chem.* **1989**, *93*, 3552–3557.
- (8) Davis, S. R.; Liu, L. *J. Phys. Chem.* **1993**, *97*, 3690–3696.
- (9) Smardzewski, R. R.; Fox, W. B. *J. Phys. Chem.*, **1975**, *79*, 219–222.
- (10) Kuo, J. C.; DesMarteau, D. D.; Fateley, W. G.; Hammaker, R. M.; Marsden, C. T.; Witt, J. D. *J. Raman Spectrosc.* **1980**, *9*, 230–238.
- (11) Brown, H. C.; Pimentel, G. C. *J. Chem. Phys.* **1958**, *29*, 883–888.
- (12) Burnett, J. K.; Poliakoff, M.; Turner, J. J.; Dubost, H. In *Advances in Infrared and Raman Spectroscopy*; Clark, R. J. H., Hester, R. E., Eds.; Heyden: London, 1976; Vol. 2.
- (13) Pacansky, J.; Coufal, H. *J. Chem. Phys.* **1980**, *72*, 3298–3303.
- (14) Brosset, P.; Dahoo, R.; Gauthier-Roy, B.; Abouaf-Marguin, L. *Chem. Phys.* **1993**, *172*, 315–324.
- (15) Risgin, O.; Taylor, R. C. *Spectrochim. Acta* **1959**, *12*, 1036–1050.
- (16) Edgell, W. F.; Riethof, T. R.; Ward, C. *J. Mol. Spectrosc.* **1963**, *11*, 92–107.
- (17) Berney, C. V. *Spectrochim. Acta* **1969**, *25A*, 793–809.
- (18) Walker, N.; Tevault, D. E.; Smardzewski, R. R. *J. Chem. Phys.* **1978**, *69*, 564–568.
- (19) J. J. Klaassen and S. R. Leone, personal communication.
- (20) Smardzewski, R. R.; Fox, W. B. *J. Am. Chem. Soc.* **1974**, *96*, 304–306.
- (21) Smardzewski, R. R.; Fox, W. B. *J. Chem. Phys.* **1974**, *60*, 2104–2110.
- (22) Jacox, M. E. *J. Phys. Chem.* **1983**, *87*, 4940–4945.
- (23) Arkell, A. *J. Am. Chem. Soc.* **1965**, *87*, 4057–4062.
- (24) Jacox, M. E. *J. Mol. Spectrosc.* **1980**, *84*, 74–88.
- (25) Ogilvie, J. F.; Salares, V. R.; Newlands, M. J. *Can. J. Chem.* **1975**, *53*, 269–275.
- (26) Roebbler, J. L. *J. Phys. Chem.* **1963**, *67*, 2391–2397.
- (27) Andrews, L.; Johnson, G. L. *J. Phys. Chem.* **1984**, *88*, 5887–5893.
- (28) Dellepiane, G.; Overend, J. *Spectrochim. Acta* **1966**, *22*, 593–614.
- (29) Schriver, L. *J. Chem. Soc., Faraday Trans. 2* **1989**, *85*, 607–621.
- (30) Pacansky, J.; Waltman, R. J.; Ellinger, Y. *J. Phys. Chem.* **1994**, *98*, 4787–4792.
- (31) Ottavianelli, E.; Maluendes, S.; Castro, E.; Jubert, A. *J. Mol. Struct.* **1990**, *69*, 305–310.
- (32) Ter Brake, J.; Driessen, R. A. J.; Mijlhoff, F. C.; Renes, G. H.; Lowrey, A. H. *J. Mol. Struct.* **1982**, *81*, 277–282.
- (33) Loos, K. R.; Lord, R. C. *Spectrochim. Acta* **1965**, *21*, 119–125.
- (34) Berney, C. V. *Spectrochim. Acta* **1971**, *27A*, 663–672.
- (35) Dune, R. A. *Canad. J. Phys.* **1966**, *44*, 337–352.
- (36) Miller, J. H.; Andrews, L. *Inorg. Chem.* **1979**, *18*, 988–992.
- (37) Bach, S. B. H.; Ault, B. S. *J. Phys. Chem.* **1984**, *88*, 3600–3604.
- (38) Loomis, R. A.; Klaassen, J. J.; Lindner, J.; Christopher, P. G.; Leone, S. R. *J. Chem. Phys.* **1997**, *106*, 3934–3947.